19th Brazilian Congress of Thermal Sciences and Engineering
November 06th-10th, 2022, Bento Gonçalves - RS - Brazil

ENC-2022-0089
PARAMETRIC STUDY OF EMPIRICAL CONSTANTS USED IN SOOT FORMATION MODELS BASED ON INTERPOLATIVE CLOSURE METHODS OF MOMENTS

Sebastián Ruiz, Sebastián Valencia, Cesar Celis
Mechanical Engineering Section, Pontificia Universidad Católica del Perú
Av. Universitaria 1801, San Miguel, Lima 32, Lima, Peru
sebastian.ruiz@pucp.edu.pe, svalenciar@pucp.edu.pe, ccelis@pucp.edu.pe

Luís Fernando Figueira da Silva
Institut Pprime UPR 3346 CNRS, ENSMA and Université de Poitiers
86961 Futurescope Chasseneuil, France
luis-fernando.figuerira-da-silva@ensma.fr

Abstract. *One of the most widely used approaches for modeling soot formation in laminar and turbulent flames is the one based on the method of moments (MOM). In particular, the method of moments with interpolative closure (MOMIC) is one of the most employed soot models nowadays. MOMIC describes the soot particle distribution function through its first moments, being the moment zero related to the soot number density and the moment one related to the soot volume fraction. Since MOMIC was originally developed for specific fuels or flame configurations only, it is necessary to adjust some of its empirical model constants when using it in different contexts. Accordingly, this work studies parametrically two empirical constants used in MOMIC soot models. That is, the sticking coefficient used in the soot nucleation stage, and the steric factor employed in the soot surface growth and oxidation stages. The MOMIC soot model accounted for in this work is implemented using ANSYS-Fluent user-defined functions (UDF). The flame configuration accounted for here for comparison and validation purposes is an ethylene laminar diffusion flame experimentally characterized in the past. The KM2 (KAUST Mech 2) chemical kinetic mechanism featuring 202 chemical species and 1351 reactions is used for describing the gas phase chemistry. Radiation effects are accounted for using the discrete ordinates method (DOM) and computing the associated absorption coefficient from a WSGG model. The main results obtained here indicate that fine-tuning the two MOMIC parameters analyzed here it is possible to describe reasonably well soot formation processes in laminar diffusion flames. Besides, it is found that the sticking coefficient has a direct effect on the amount of soot produced, whereas the steric factor influences not only the amount of soot produced, but also the location of the soot volume fraction peak values.*

Keywords*: Soot modeling, Detailed kinetic mechanisms, Soot precursors, PAH, Diffusion flames.*

1. INTRODUCTION

The combustion of hydrocarbon (HC) based fuels is present in many important domestic and industrial applications. The referred combustion processes produce many pollutants including particulate matter or soot, which is known for its negative impacts on both health and environment. For instance, according to a WHO (World Health Organization) study, almost 4 million deaths per year are caused by inefficient and poorly ventilated combustion processes employed in domestic buildings (Pope et al., 2021). Moreover, soot is linked to respiratory, cardiovascular and carcinogenic diseases (Niranjan and Thakur, 2017). In addition, soot is a material that effectively absorbs solar radiation and thus, when deposited on surfaces, causes local heating of the environment (He, 2019; Lohmann et al., 2020). Another negative impact of soot is that it alters the cloud formation process, acting as a condensation nucleus (Wang, 2011). The study of soot is also motivated by the need to optimize HC combustion systems and fill the knowledge gaps of the physical and chemical mechanisms controlling soot formation (Valencia et al., 2021a). In this context lies the importance of using computational fluid dynamics (CFD) based approaches and the development and use of soot formation models that can properly predict soot formation under different reactive flow conditions.

CFD-based numerical modeling of soot formation in laminar flames typically involves the use of several chemical and physical models, each representing a significant amount of computational cost. Namely, the solution of (i) the stiff

detailed chemistry, which involves the estimation of hundreds of chemical species and thousands of chemical reactions, (ii) the detailed soot model accounting for soot dynamics related processes, and (iii) the detailed radiation model, affecting the heat transfer and temperature transport, which the previously mentioned models are sensitive to. State-of-the-art soot formation models are often classified as deterministic or stochastic (Rigopoulos, 2019). Since a large soot number density characterizes soot formation processes, tracking each soot particle results in a relatively high computational cost, and the use of stochastic methods is generally restricted to simplified 1-D laminar flame configurations (Wick et al., 2020). Deterministic models include the method of moments and the sectional method, whose most used variants include the MOM with interpolative closure (MOMIC) and the discrete sectional method (DSM). Although MOMIC is not considered as being as accurate as the DSM, it has a relatively low computational cost, needing the solution of only a few (generally three) additional transport equations to obtain the PSDF (soot particle size distribution function) (Valencia et al., 2021a).

MOMIC was initially developed for (methane) laminar premixed flames (Frenklach, 2002), so for diffusion flames the model empirical parameters need to be properly modified. Accounting for different flame configurations, numerous studies have been carried out in the past where the referred model empirical parameters have been modified to properly reproduce the reference data employed. One of the model parameters that has been modified in the past is the reaction rate for one of the soot surface growth reactions. For instance, to properly reproduce soot peak values in laminar diffusion flames, Guo et al. (2004) and Dasgupta et al. (2014) tested different values for this parameter. Seeking to reduce soot concentration, another common modification involves the use of an efficiency factor in the source term present in the PAH (polycyclic aromatic hydrocarbon) condensation model (Zhang et al., 2009; Dworkin et al., 2006). However, one of the parameters with a marked influence on the soot levels is the steric factor α present in both source terms of surface growth and oxidation. In this sense, Frenklach and Wang (1994) used a constant value, whereas Appel et al. (2000) used a fitted correlation, where α was a function of the local temperature and the average soot particle size. Another factor with a relatively large effect on soot peak values is the sticking factor present in the soot nucleation stage, which is employed to decrease the nucleation rate assuming a collision efficiency between precursors (Blanquart and Pitsch, 2009).

Accordingly, the objective of this work is to parametrically study some of the model parameters to improve MOMIC soot predictions in a non-premixed, two-dimensional configuration. The results from this work allow having a better understanding of these model parameters and their influence on soot predictions. A laminar diffusion ethylene/air flame experimentally characterized in the past (Jerez et al., 2019) is used as a reference flame here. This flame configuration has been chosen because it allows the analysis of different aspects of soot formation. Some of its assets are that the main physical and chemical soot-related phenomena are present, soot is formed in relatively high quantities, and a 2D axisymmetric scheme is accounted for (Kholgy et al., 2013). This work is structured as follows. The mathematical models considered here are first described in Section 2. In Section 3, the flow configuration and the numerical methods utilized are summarized. In Section 4, the main results of the parametric study carried out here are presented and discussed. Finally, the main outcomes from this work are summed up in Section 5.

2. MATHEMATICAL MODELING

In this section the main characteristics of the mathematical models employed in this work are described. Governing equations accounted for are firstly presented. The chemical kinetic mechanism, MOMIC and the radiation models used here are also discussed. Further details about the models employed here can be found in Valencia et al. (2021b) and Ruiz et al. (2021).

2.1. Governing equations

A laminar coflow diffusion flame is accounted for in this work. Accordingly, transport equations for mass, momentum, energy, and chemical species are solved considering laminar flows with variable density and an axisymmetric reference frame.

2.2. Gas phase kinetic mechanism

The chemical source terms for the species conservation equations are computed from the Kaust-Mech 2 (KM2) chemical kinetic mechanism (Wang et al., 2013). This mechanism includes 202 chemical species and 1351 chemical reactions. In the KM2, a previously validated kinetic mechanism for C1-C4 fuels, known as USCII (Wang et al., 2007), is used as a base for the description of the main reaction paths regarding the molecular growth up to the first aromatic ring. This mechanism also features an upgrade on cyclopentadienyl related reactions, accounting for its influence on the formation of PAH. H-abstraction mechanism on important aliphatic and aromatic molecules enabling further reactions is also accounted for. Lastly, the main advantage of the KM2 is that it describes in detail the PAH growth up to coronene ($C_{24}H_{12}$).

2.3. Soot models

The method of moments utilized here uses a Lagrange interpolation for the closure of the moments-related source terms (Frenklach, 2002). When using this model, the steps in soot evolution are modeled as follows. Soot nucleation

involves the coalescence of PAH, coagulation features the collision and union of two particles, and surface growth and oxidation include in turn surface reactions of soot with acetylene, hydroxyl radical and molecular oxygen. Specifically, for each moment, a transport equation of the form,

$$\frac{\partial \rho(M_r)}{\partial t} + \nabla \cdot (\rho \bar{v}) M_r = \nabla \cdot (D_s \nabla M_r) + \frac{dM_r}{dt}, \tag{1}$$

is solved, in which the different referred soot evolution mechanisms are accounted for. In Eq. (1), M_r stands for the r-th moment of the soot size distribution, and D_s is the diffusion coefficient for the moment transport equation (1.0E-06). Finally, dM_r/dt is the r-th moment source term. This last term is in turn computed as follows,

$$\frac{\mathrm{d}M_r}{dt} = R_r + G_r + W_r. \tag{2}$$

where R_r, G_r and W_r are the inception, coagulation, and surface growth and oxidation source terms, respectively. Notice that the zeroth moment M_0 accounts for nucleation and coagulation source terms only. Higher order moments provide a more accurate description of the particle size distribution, accounting for all three R, G and W source terms. For full description of each of these source terms, the interested reader may refer to the works by Frenklach (2002) and Rigopoulos (2019).

Soot nucleation (R_r) is usually modeled as a coagulation between two PAH molecules. In this work, due to both its simplicity and the fact that it does not need additional moments equations as other models do so (Frenklach and Wang, 1994), the formulation proposed by Rezvan et al. (2002) is utilized, and the four-ring PAH (pyrene) is considered here as soot precursor specie. The nucleation source term for the zeroth moment is,

$$R_0 = \gamma \sqrt{\frac{4\pi k_B T}{m_C N_{C,P}}} (dN_A)^2 [PAH]^2, \tag{3}$$

where m_C is the mass of a carbon atom, NC_{PAH} is the number of carbon atoms in a PAH molecule, d_{PAH} is the diameter of the PAH molecule, N_{PAH} is the number density of the PAH molecule, k_B is the Boltzmann constant, and γ is the sticking coefficient, which is one of the study objectives in this work. The source terms for higher-order moments are of the form $R_r = 2N_{C,P}R_{r-1}$.

Soot coagulation (G_r) is based on the Smoluchowski equations (Smoluchowski, 1917), where the collision coefficient is described for all coagulation regimes, free molecular, continuum and transition. These regimes are classified as a function of the Knudsen number, $k_n = \lambda/d_s$, where λ is the gas mean free path and d_s is the soot particle diameter (Kazakov and Frenklach, 1998). Further details about this formulation are given in Valencia et al. (2021a).

Surface growth and oxidation (W_r) are modeled using the hydrogen abstraction C_2H_2 addition mechanism (HACA) (Frenklach and Wang, 1994). In the HACA mechanism, the reactions rates are computed using Arrhenius form equations employing the rate coefficients summarized by Appel et al. (2000). The surface growth rate due to C_2H_2 and the oxidation rates due to O_2 and OH are computed, respectively, as follows,

$$W_r^{C_2H_2} = k_4[C_2H_2]\, \alpha \chi C_{soot} \circ \pi {C_s}^2 M_0 \sum_{l=0}^{r-1} (r\ l)\mu_{l+\frac{2}{3}} (2)^{r-l}, \tag{4}$$

$$W_r^{O_2} = k_5[O_2]\, \alpha \chi C_{soot} \circ \pi {C_s}^2 M_0 \sum_{l=0}^{r-1} (r\ l)\mu_{l+\frac{2}{3}} (-2)^{r-l}, \tag{5}$$

$$W_r^{OH} = \gamma_{OH}[OH] \sqrt{\frac{\pi k_b T}{2m_{oh}}} N_A {C_s}^2 M_0 \sum_{l=0}^{r-1} (r\ l)\mu_{l+\frac{2}{3}} (-1)^{r-l}, \tag{6}$$

where k_4 and k_5 are the kinetic rate coefficients for reactions with C_2H_2 and O_2, respectively. Also $[C_2H_2]$, $[O_2]$ and $[OH]$ stand for molar concentrations of gas species, γ_{OH} is the collision efficiency for the OH radical, m_{oh} is the mass of an OH radical, C_s is the particle diameter, $\chi C_{soot} \circ$ is the number density of the surface radicals, and α is the steric factor. According to the Appel et al. (2000) formulation, the steric factor is computed as,

$$\alpha = \tanh\left[\frac{a}{\log\left({M_1}/{M_0}\right)} + b\right], \tag{7}$$

where a and b are both function of temperature, and they are determined from,

$$a = 12.65 - 0.00563\,T, \tag{8}$$

$$\mathrm{b} = -1.38 + 0.00068\,T. \tag{9}$$

2.4. Radiation models

The solution of the RTE (radiative transfer equation) in this work is carried out by using the discrete ordinates method (DOM). This model involves the solution of a transport equation for each direction vector determined by the angular discretization. Additionally, assuming an optically thin medium and neglecting the effects of scattering phenomena, radiation properties, such as the total gas emissivity and absorption coefficients, are computed with the weighted sum of gray gases (WSGG) model (Yadav et al., 2013).

3. NUMERICAL APPROACH

In this section the main features of the numerical approach employed in this work are briefly described.

3.1 Case study

The flame configuration accounted for in this work corresponds to a laminar ethylene/air diffusion flame stabilized in a coflow. The fuel flow is conducted through a 10.65mm diameter duct, whereas the air coflow is limited by a 99.90mm diameter outer duct. The inlet fuel flow rate is set to 0.1 slpm, whereas the inlet air flow rate value is 60 slpm. Additionally, air composition corresponds to normal conditions, where N_2 and O_2 are present at 79% and 21% (molar fraction), respectively. The experimental data used here for comparison purposes was obtained by Jerez et al. (2019), where soot volume fraction and other soot related parameters were measured. More specifically, measurements were carried out by simultaneous laser induced incandescence (LII) and planar laser induced fluorescence (PLIF) techniques. In turn, measurements of temperature fields were performed by means of a two color pyrometry technique. Further details on boundary conditions accounted for in this work are found in Ruiz et al. (2021).

3.2 Numerical setup

In this work ANSYS Fluent (ANSYS, 2021a) was used to solve the set of governing equations indicated in Section 2. The stiff chemistry solver was employed to obtain species reaction rates and mean gas phase properties. The discrete ordinates model (DOM) used for the solution of the RTE features a 4x4 quadrature. MOMIC transport equations were accounted for using user-defined scalars (UDS), whereas user-defined functions (UDF) were developed for both the definition of source terms and the absorption coefficient model. Regarding numerical methods, a second-order upwind scheme was used for all transport equations, and a least squares cell-based method was used for gradients and derivates evaluation. PRESTO! scheme and PISO algorithm were used for pressure interpolation and velocity-pressure coupling, respectively. The mesh utilized here corresponds to a one that was used previously, which was refined through mesh adaptions based on global scaled gradients of specific gaseous chemical species, i.e., C_2H_6, C_3H_3 and OH (Da Costa et al., 2022; Ruiz et al., 2021). For these mesh adaptions, normalized threshold values in the range between 0.1 and 0.01 were chosen according to the results obtained progressively. The employed mesh consists of almost 90,000 elements, where the smallest element has a size of approximately 30μm.

4. RESULTS AND DISCUSSION

In this section, the main results obtained here are presented and discussed. More specifically, the results from the evaluation and analysis of two selected MOMIC parameters carried out are firstly described. Next, temperature and soot volume fraction profiles obtained using MOMIC are compared with both experimental data and other numerical results coming from a detailed soot model.

4.1 Integrated soot formation parametric study

Although MOMIC describes the soot evolution process using physical and chemical principles, there are a number of empirical factors and parameters that need fine-tuning to reproduce the experimental data characterizing different flame configurations. Two model parameters frequently modified are the sticking coefficient (γ) used to describe the soot nucleation [Eq. (3)] and the steric factor (α) present in the expressions used to model both surface growth and O_2 oxidation processes [Eq. (4) and Eq. (5)]. First, the sticking coefficient was introduced to account for higher values of collision rates coming from the kinetic theory of gasses (Blanquart and Pitsch, 2009). In turn, the steric factor is defined as the fraction of active sites available for surface reactions. This factor was introduced to account for the change in the particle's morphology during its evolution (maturation) and the fact that there are unreactive planes on its surface (Appel et al., 2000). The steric factor has been shown to be a function of temperature and particle size. However, there are also several

past works that have employed a constant value for this factor and carried out acceptable soot predictions (Eaves et al., 2016; Jerez et al., 2019).

The parameter used in this work to analyze the sensibility of the soot predictions to the mentioned model parameters is the radially integrated soot volume fraction. This parameter has been computed in this work as follows,

$$\beta = 2\pi \int r\, f_{v-soot}\, dr \tag{10}$$

where r is the radial coordinate and f_{v-soot} is the soot volume fraction. This β parameter represents a convenient way to evaluate soot model parameters in a 2D axisymmetric flame configuration.

Accordingly, Figure 1 shows the radially integrated soot volume fraction β axial profiles obtained for different values of the sticking coefficient γ. The results shown in this figure were obtained using the Appel et al. (2000) steric factor [Eq. (7)]. It is observed from Figure 1 that, although the sticking coefficient does not influence so much the height above the burner at where the soot quantity peaks, it does directly affect the amount of soot produced. Particularly, the sticking coefficient value that brought the numerical result as close as possible to the experimental integrated soot volume fraction was in the range between 0.001 and 0.01. From the comparisons of the maximum values of β, it seems that there is a higher sensibility of the soot predictions to the sticking coefficient values in the range between 0.001 and 0.01 as well. This may be because, as the number of particles increases, surface reaction mechanisms also become more significant.

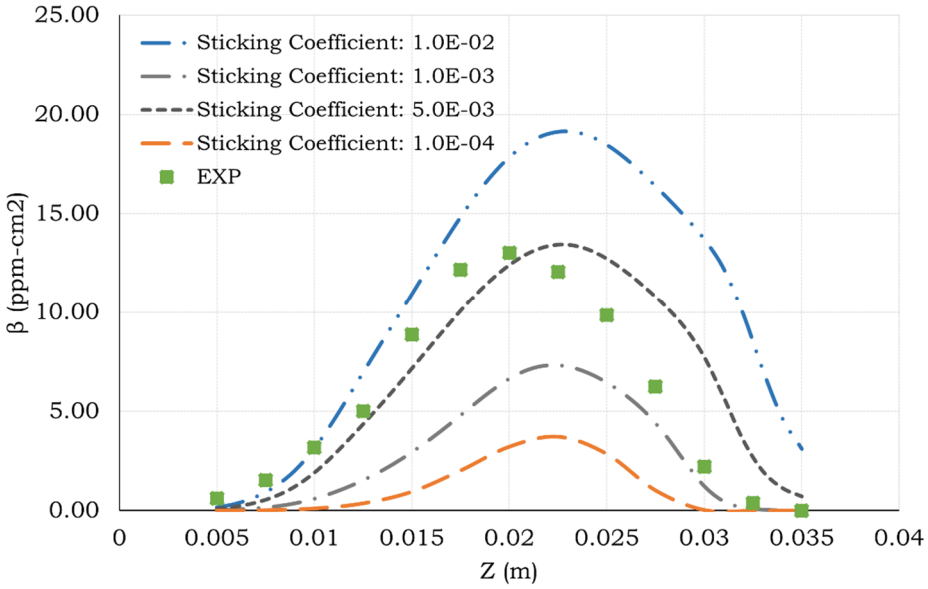

Figure 1. Axial profiles of radially integrated soot volume fraction (β) for different sticking coefficients (γ). Square symbols correspond to experimental data by Jerez et al. (2019).

Similarly, Figure 2 shows the radially integrated soot volume at several heights above the burner for different constant values of steric factor and for α values coming from the expression proposed by Appel et al. (2000) [Eq. (7)]. Notice that the results shown in this figure were computed considering a constant sticking coefficient value equal to 0.005. From this figure, it is observed that both constant and temperature/particle size dependent steric factors lead to soot predictions that can be fairly compared to experimental data. Moreover, the axial position (Z = 0.02m) of the β peak value associated with the experimental data is better captured when using a constant steric factor. These results seem to suggest that the influence that the steric factor has on both surface growth by C_2H_2 and oxidation by O_2 is partially responsible for the observed β peak values and the decreasing segment of the three numerically predicted β profiles. Finally, as highlighted by Valencia et al. (2021a), to predict soot formation in turbulent diffusion flames, the same soot model parameters, sticking coefficient γ and steric factor α appearing in Eqs. (3) and (7), respectively, need also to be fine-tuned to fit the experimental soot volume fraction peak values. Comparing the results described by Valencia et al. (2021a) to the ones obtained here, it is seen that the influence of the sticking coefficient on the integrated soot volume fraction β is similar in both laminar and turbulent flames, i.e., as the sticking factor decreases, the β peak values remain at the same axial position and soot concentrations decrease. The same does not occur in the case of the steric factor α. Indeed, in the turbulent case, as the value of the steric factor increases, the soot peak values decrease and shift slightly downward. In the laminar case, however, soot concentrations increase proportionally to the steric factor.

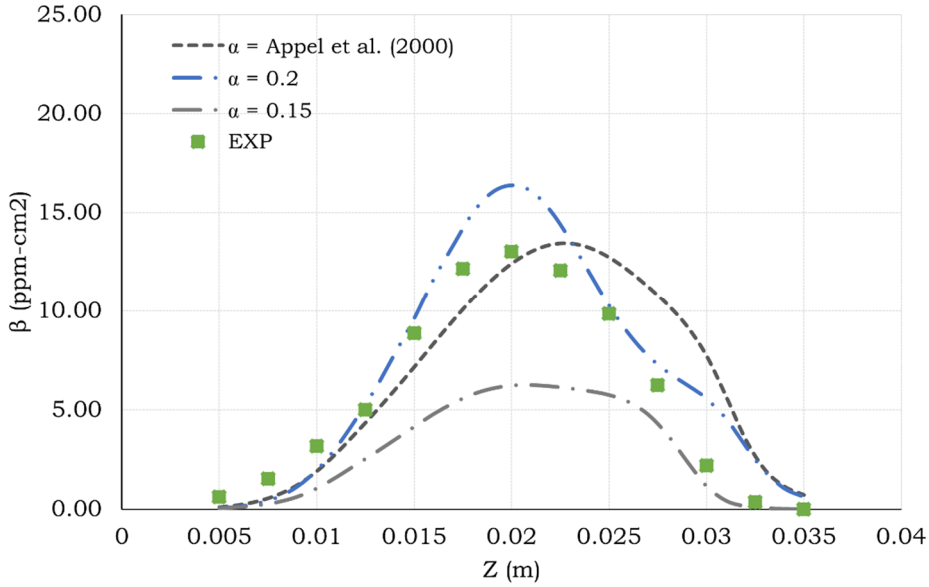

Figure 2. Axial profiles of radially integrated soot volume fraction (β) for different steric factors (α). Square symbols correspond to experimental data by Jerez et al. (2019).

4.2. Flame and soot characteristics

In this section, axial and radial profiles of temperature (Figure 3) and soot volume fraction (Figure 4) predicted here are compared to both experimental data and other numerical results available in the work by Jerez et al. (2019). The computed profiles are plotted along the flame centerline and at an axial position equal to Z= 0.01896 m, which corresponds to a flame height above the burner considered as reference here. Notice that the numerical results shown in this section were obtained accounting for a sticking coefficient equal to 0.0015 and the Appel et al. (2000) expression for computing the steric factor. It should be noticed as well that the numerical results from Jerez et al. (2019) considered for comparison purposes here were obtained using a discrete sectional method (DSM) that employs 35 additional transport equations. As indicated in Section 1, the DSM model is expected to be more accurate and the MOMIC to be less computationally expensive. In Figure 3 and Figure 4, square symbols, dotted, and dashed lines represent, respectively, experimental data (Jerez et al., 2019), DSM (Jerez et al., 2019) and MOMIC model. From Figure 3 it is observed first that the measured temperature profiles are well reproduced, both on curve shape and peak values. It is also noticed that, for both axial and radial profiles, the computed MOMIC profiles are slightly shifted to large radius values. Nevertheless, these differences are within the experimental uncertainty, which is about 16% (290 K).

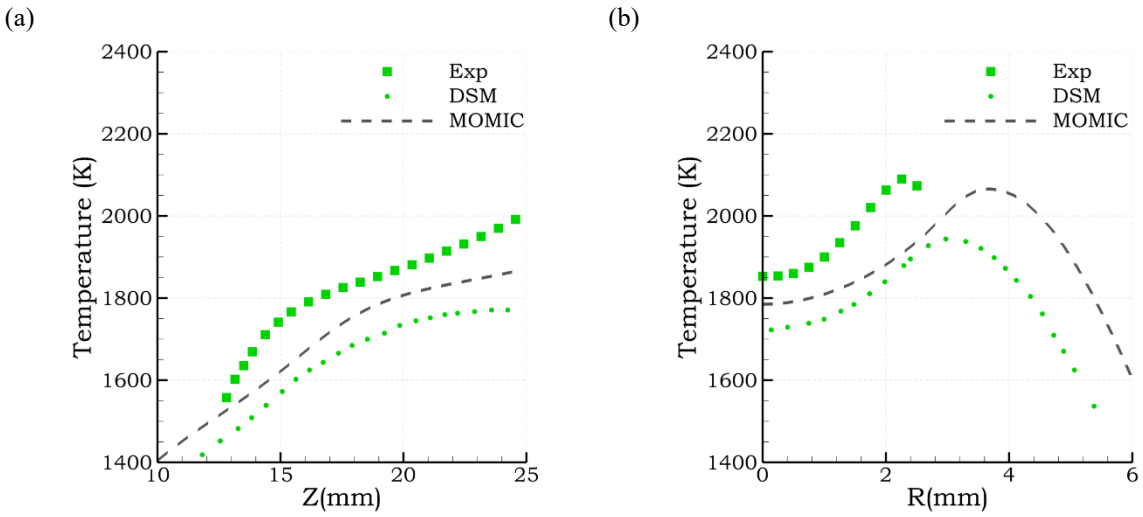

Figure 3. Temperature profiles along the flame centerline (a) and the radial direction at Z= 0.01896m (b). Exp, DSM and MOMIC correspond to, respectively, experimental data (Jerez et al., 2019), discrete sectional method (Jerez et al., 2019), and method of moments with interpolative closure.

Figure 4 shows in turn axial and radial profiles of soot volume fraction in representations analogous to those of Figure 3. Overall, it is found that, although the experimental data profiles were not exactly reproduced, fair agreement was obtained with the numerical predictions carried out. Particularly, from Figure 4a and Figure 4b, compared to the experimental ones, peak values of soot volume fraction are underpredicted by 3 ppm and 0.5 ppm, respectively. Similar to what was observed in the temperature profiles, when compared to the DSM one, Figure 4b shows that the computed MOMIC soot volume fraction profile is slightly shifted to a larger radius. Therefore, as indicated in the work by Jerez et al. (2019), since the soot nucleation and condensation mechanisms dominate in the flame central region, underprediction of the soot volume fraction along the flame centerline imply that these model mechanisms need further improvement for this type of flames.

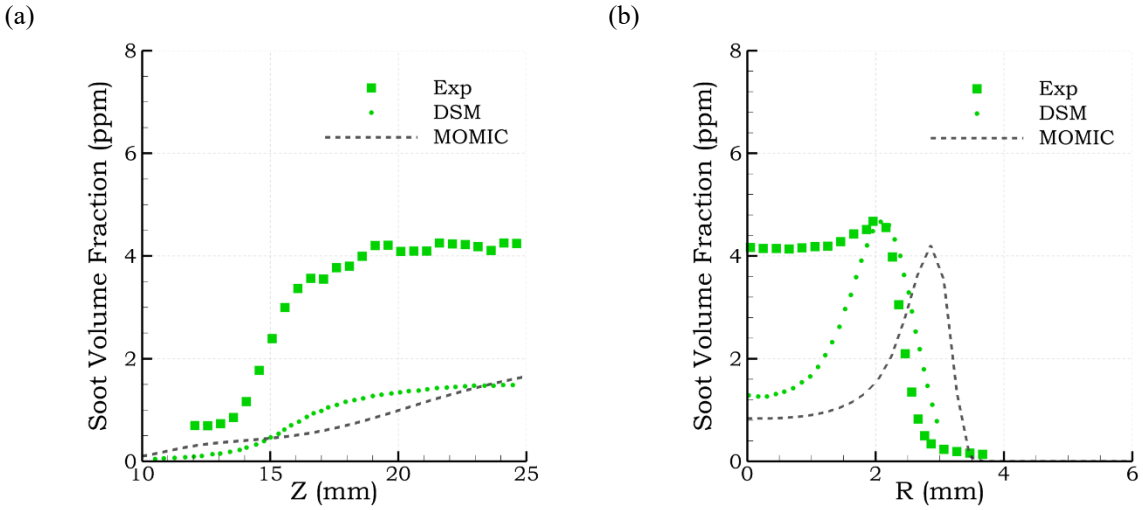

Figure 4. Soot volume fraction profiles along the flame centerline (a) and the radial direction at Z= 0.01896m (b). Exp, DSM and MOMIC correspond to, respectively, experimental data (Jerez et al., 2019), discrete sectional method (Jerez et al., 2019), and method of moments with interpolative closure.

5. CONCLUSIONS

In this work a parameter study of the sticking coefficient and the steric factor used in MOMIC soot formation models was carried out. From the obtained results it is concluded that the sticking coefficient has a direct effect on the amount of soot produced. Therefore, when used simultaneously with all soot formation mechanisms, including coagulation, surface growth and oxidation, controlling this parameter permits to obtain the correct order of magnitude of soot volume fraction. Additionally, for the laminar diffusion flame analyzed here, it was found that the steric factor influences not only the amount of soot produced, but also the location of the soot volume fraction peak value. In addition, temperature and soot volume fraction profiles predicted by MOMIC were also compared with experimental data and discrete sectional method related results. In terms of temperature, the results showed a good agreement with experimental data, as curves shape and peak values were well reproduced. As expected, in terms of soot volume fraction, DSM showed a better agreement with the reference profiles, whereas the MOMIC curves resulted slightly shifted to a larger radius. The results obtained here seem to suggest that, for the laminar flame analyzed in this work, by adding only three additional transport equations, it is possible to obtain acceptable soot predictions that fairly agree with experimental data. Discrepancies between the soot numerical predictions and the experimental data along the flame centerline emphasizes the fact that the models used for soot nucleation and condensation need to be further improved. By comparing the MOMIC empirical parameters related results discussed in this work to similar ones obtained previously for a turbulent flame, it was found that different trends characterize the influence of the steric factor on the integrated soot volume fraction. Therefore, to have an insight about the influence of these empirical parameters on soot formation in other flame configurations, future works should carry out analyses similar to those performed here.

6. ACKNOWLEDGEMENTS

This work has been supported by CONCYTEC-FONDECYT (Peru), Contract No. 415-2019-2019-FONDECYT, “Identification of soot precursors in turbulent combustion processes through numerical modeling to reduce the impact of soot on both health and environment”. During this work Luís Fernando Figueira da Silva was on leave from the Pontificia Universidade Catolica de Rio de Janeiro (PUC-Rio, Brazil).

7. REFERENCES

ANSYS Fluent, 2021. ANSYS Inc., https://www.ansys.com/products/fluids/ansys-fluent. Accessed 21 June 2021.

Appel, J., Bockhorn H., and Frenklach M., 2000. "Kinetic Modeling of Soot Formation with Detailed Chemistry and Physics: Laminar Premixed Flames of C2 Hydrocarbons." *Combustion and Flame* 121(1–2):122–36.

Blanquart, G., and Pitsch, H., 2009. "A joint volume-surface-hydrogen multi-variate model for soot formation." Combustion Generated Fine Carbonaceous Particles, 437-463.

Da Costa Ramos, L., Figueira da Silva, L., F., Di Meglio, F., and Morgenthaler, V. 2022. "Modelling of pulsating inverted conical flames: a numerical instability analysis". *Combustion Theory and Modelling* 26:2, 260-288

Dasgupta, A., Roy, S., and Haworth, D. C., 2014. "Detailed computational modeling of laminar and turbulent sooting flames". *ACM International Conference Proceeding Series* 12:1–7.

Dworkin, S. B., Bennett, B. A. V, and Smooke, M. D., 2006. "A mass-conserving vorticity – velocity formulation with application to nonreacting and reacting flows". *Journal of Computational Physics*133:430–447.

Eaves, N. A., Zhang, Q., Liu, F., Guo, H., Dworkin, S. B., & Thomson, M. J., 2016. CoFlame: A refined and validated numerical algorithm for modeling sooting laminar coflow diffusion flames. *Computer Physics Communications*, *207*.

Frenklach, M., and Wang, H., 1994. "Detailed mechanism and modeling of soot particle formation". *Springer Series in Chemical Physics* 59:165–192.

Frenklach, M., 2002. "Method of Moments with Interpolative Closure." *Chemical Engineering Science* 57(12):2229–39.

Guo, H., Liu, F., and Smallwood, G. J., 2004. "Soot and NO formation in counterflow ethylene/oxygen/nitrogen diffusion flames". *Combustion Theory and Modelling* 8:475–489.

He, C., 2019. Radiative Properties of Atmospheric Black Carbon (Soot) Particles with Complex Structures. *Springer Series in Light Scattering.* https://doi.org/10.1007/978-3-030-20587-4_5

Jerez, A., Cruz, J.J., Figueira da Silva L.F., Demarco, R., and Fuentes, A., 2019. "Measurements and Modeling of PAH Soot Precursors in Coflow Ethylene/Air Laminar Diffusion Flames." *Fuel* 236:452–60.

Kazakov, A., and Frenklach, M., 1998. "Dynamic modeling of soot particle coagulation and aggregation: Implementation with the method of moments and application to high-pressure laminar premixed flames". *Combustion and Flame* 114:484–501.

Kholghy, M., Saffaripour, M., Yip, C., and Thomson, M. J., 2013. The evolution of soot morphology in a laminar coflow diffusion flame of a surrogate for Jet A-1. *Combustion and Flame*, *160*(10), 2119–2130.

Lohmann, U., Friebel, F., Kanji, Z. A., Mahrt, F., Mensah, A. A., and Neubauer, D., 2020. Future warming exacerbated by aged-soot effect on cloud formation. *Nature Geoscience*, *13*(10), 674–680.

Niranjan, R., and Thakur, A. K., 2017. The toxicological mechanisms of environmental soot (black carbon) and carbon black: Focus on Oxidative stress and inflammatory pathways. *Frontiers in Immunology*, *8*(JUN), 1–20.

Pope, D., Johnson, M., Fleeman, N., Jagoe, K., Duarte, R., Maden, M., Ludolph, R., Bruce, N., Shupler, M., Adair-Rohani, H., and Lewis, J., 2021. Are cleaner cooking solutions clean enough? A systematic review and meta-analysis of particulate and carbon monoxide concentrations and exposures. *Environmental Research Letters*, *16*(8).

Rezvan, K. L., Brown, N. J., and Frenklach, M., 2002. "Soot formation codes," http://combustion.berkeley.edu/soot/codes/codes.html . Accessed 21 June 2021.

Rigopoulos, S., 2019. "Modelling of Soot Aerosol Dynamics in Turbulent Flow." *Flow, Turbulence and Combustion* 103(3): 565–604.

Ruiz, S., Celis, C., Figueira da Silva, L. F., 2021. "Soot precursors analysis using detailed chemical kinetic mechanisms in an ethylene/air diffusion flame". In *26th International Congress of Mechanical Engineering – COBEM 2021*. Online.

Smith, T. F., Shen, Z. F., and Friedman, J. N., 1982. "Evaluation of Coefficients for the Weighted Sum of Gray Gases Model." *Journal of Heat Transfer* 104(4):602–8.

Smoluchowski, M., 1917. "Mathematical theory of the kinetics of coagulation of colloidal systems". *Z. Phys. Chem,* 9:129–168.

Valencia, S., Ruiz, S., Manrique, J. Celis, C., Figueira da Silva, L. F., 2021a. Soot modeling in turbulent diffusion flames: review and prospects. *J Braz. Soc. Mech. Sci. Eng.* 43**,** 219

Valencia, S., Celis, C., Figueira da Silva, L. F., 2021b. "Application of a soot formation model based on an interpolative closure method of moments to a turbulent non-premixed flame". In *26th International Congress of Mechanical*

Engineering – COBEM 2021. Online.

Wang H., You, X., Joshi, A.V., Davis, S.G., Laskin, A., Egolfopoulos, F., and Law, C.K., 2007. "USC Mech Version II. High-Temperature Combustion Reaction Model of H2/CO/C1-C4 Compounds."

Wang, H., 2011. Formation of nascent soot and other condensed-phase materials in flames. *Proceedings of the Combustion Institute*, *33*(1), 41–67. https://doi.org/10.1016/j.proci.2010.09.009

Wang, Y., Raj, A., and Chung, S. H., 2013. "A PAH Growth Mechanism and Synergistic Effect on PAH Formation in Counterflow Diffusion Flames." *Combustion and Flame* 160(9):1667–76.

Wick, A., Frenklach, M., and Pitsch, H., 2020. "Systematic assessment of the Method of Moments with Interpolative Closure and guidelines for its application to soot particle dynamics in laminar and turbulent flames". *Combustion and Flame*, Vol. 214, pp. 450-463

Yadav, R., Kushari, A., Verma, A. K., and Eswaran, V., 2013. "Weighted Sum of Gray Gas Modeling for Nongray Radiation in Combusting Environment Using the Hybrid Solution Methodology." *Numerical Heat Transfer, Part B: Fundamentals* 64(2):174–97.

Zhang, Q., H. Guo, F. Liu, G. Smallwood, and M. Thomson, 2009. "Modeling of soot aggregate formation and size distribution in a laminar ethylene/air coflow diffusion flame with detailed PAH chemistry and an advanced sectional aerosol dynamics model," Proceedings of the Combustion Institute, 32(1):761 – 768.

8. RESPONSIBILITY NOTICE

The authors are the only responsible for the printed material included in this paper.